Inorg. Chem. **2009**, *48*, 4542−4548

Bonding Characteristics, Thermal Expansibility, and Compressibility of RXO_4 (R = Rare Earths, X = P, As) within Monazite and Zircon Structures

Huaiyong Li,[†,‡] Siyuan Zhang,[*,†] Shihong Zhou,[†] and Xueqiang Cao[†]

State Key Laboratory of Rare Earth Resource Utilization, Changchun Institute of Applied Chemistry, Chinese Academy of Sciences, Changchun 130022, P. R. China, and Graduate School, Chinese Academy of Sciences, Beijing 100049, P.R. China

Received February 19, 2009

Systematically theoretical research was performed on the monazite- and zircon-structure RXO_4 (R = Sc, Y, La, Ce, Pr, Nd, Sm, Eu, Gd, Tb, Dy, Ho, Er, Tm, Yb, Lu; X = P, As) series by using the chemical bond theory of dielectric description. The chemical bond properties of R−O and X−O bonds were presented. In the zircon phase, the covalency fractions of X−O bonds increased in the order of V−O < As−O < P−O, which was in accordance with the ionic radii and electronegative trends, and the covalency fractions of R−O bonds varied slightly due to the lanthanide contraction. While in the monazite phase, both R−O and X−O bonds were divided into two groups by their covalency fractions. The contributions from the bond to the lattice energy, linear thermal expansion coefficient (LTEC), and bulk modulus were explored. The X−O bonds with short bond lengths and high chemical valence made greater contributions to the lattice energy and performed nearly rigidly during the deformation. A regular variation of lattice energy, LTEC, and bulk modulus with the ionic radii of the lanthanides was observed in both monazite and zircon phases.

1. Introduction

Rare earth orthophosphates, orthoarsenates, and orthovanadates with the general formula RXO_4 (R = rare earths and X = P, As, or V) constitute a big family. In this family, the compounds generally crystallize in two different structural types depending on the radius ratio of ions on R and X sites. The compounds containing rare earths with large ionic radii, namely, orthophosphates RPO_4 with R = La, Ce, Pr, Nd, Sm, Eu, and Gd, as well as orthoarsenates $RAsO_4$ with R = La, Ce, Pr, and Nd, crystallize in the monoclinic monazite structure, whereas those containing rare earths with small ionic radii, namely, RPO_4 (R = Tb, Dy, Ho, Er, Tm, Yb, Lu, Y, Sc) and $RAsO_4$ (R = Sm, Eu, Gd, Tb, Dy, Ho, Er, Tm, Yb, Lu, Y, Sc), crystallize in the tetragonal zircon (or xenotime) structure, and all of the rare earth orthovanadates crystallize in the zircon structure. The members of this family have gained increasing attention in the past few decades due to their wide potential application and interesting properties:[1] The luminescence properties of adopted RVO_4 and RPO_4 are extensively studied,[2−9] and YVO_4:Nd is one of the most important diode-pumped solid-state lasers. RPO_4, as well as $RAsO_4$, have been proposed as potential nuclear waste matrixes due to their high melting points and resistance to damage. $LaPO_4$ has been expected as a candidate for high-temperature composite ceramics with its excellent high-temperature properties and comparable thermal expansion coefficient versus that of Al_2O_3.[10,11] Investigations of the

* To whom correspondence should be addressed. Fax: +86 431 85698041. Tel.: +86 431 85262043. E-mail: syzhang@ciac.jl.cn.
† Changchun Institute of Applied Chemistry.
‡ Graduate School, Chinese Academy of Sciences.

(1) Kolitsch, U.; Holtstam, D. *Eur. J. Mineral.* **2004**, *16*, 117.
(2) Buissette, V.; Moreau, M.; Gacoin, T.; Boilot, J.-P.; Chane-Ching, J.-Y.; Le Mercier, T. *Chem. Mater.* **2004**, *16*, 3767.
(3) Jüstel, T.; Huppertz, P.; Mayr, W.; Wiechert, D. U. *J. Lumin.* **2004**, *106*, 225.
(4) Ng, S. L.; Lam, Y. L.; Zhou, Y.; Ooi, B. S.; Kam, C. H.; Wong, K. S.; Rambabu, U.; Buddhudu, S. *J. Mater. Sci. Lett.* **2000**, *19*, 495.
(5) Yan, B.; Su, X.; Zhou, K. *Mater. Res. Bull.* **2006**, *41*, 134.
(6) Rambabu, U.; Buddhudu, S. *Opt. Mater.* **2001**, *17*, 401.
(7) Xiu, Z.; Yang, Z.; Mengkai, L.; Liu, S.; Zhang, H.; Zhou, G. *Opt. Mater.* **2006**, *29*, 431.
(8) Hernández, T.; Martı´n, P. *J. Alloys Compd.* **2008**, *466*, 568.
(9) Hernández, T.; Martı´n, P. *J. Eur. Ceram. Soc.* **2007**, *27*, 109.
(10) Morgan, P. E. D.; Marshall, D. B. *J. Am. Ceram. Soc.* **1995**, *78*, 1553.
(11) Min, W.; Miyahara, D.; Yokoi, K.; Yamaguchi, T.; Daimon, K.; Hikichi, Y.; Matsubara, T.; Ota, T. *Mater. Res. Bull.* **2001**, *36*, 939.

10.1021/ic900337j CCC: $40.75
Published on Web 03/26/2009

thermal, mechanical, and chemical properties of RPO_4 and $RAsO_4$ have made a dent in recent years. Systematical variations of thermal and mechanical properties with rare earth ionic radii were explored in the RPO_4 series.[12−14] However, theoretical research of the bonding characteristics and their determination of the thermal and mechanical properties of this family were seldom reported.[15,16] We believe that the thermal and mechanical properties of the crystals depend strongly on their structure and bonding characteristics. And, the resistance to amorphization of a complex crystal was also suggested to be relevant to the covalency of bonding.[17] We were excited to perform an investigation on the bonding characteristics and their determination of the expansibility and compressibility in RPO_4 and $RAsO_4$ series.

In this paper, we will report a systematical investigation on the chemical bond properties, thermal expansibility, and compressibility of monazite- and zircon-type rare earth orthophosphates and orthoarsenates by using the chemical bond theory of dielectric description. In the following section, we will give a brief introduction of the theoretical method. In the third part, the covalency fractions of $R^{3+}-O$ and $P(As)^{5+}-O$ bonds will be first introduced; their characteristics will be discussed on the basis of the coordination number, chemical valence, ionic radii, and electronegativity. And then, the contributions to the lattice energy, linear thermal expansion coefficient (LTEC), and bulk modulus from individual bonds will be estimated. The relationship between microstructure and thermal expansibility, as well as compressibility, will be discussed. Finally, the calculated lattice energies, LTECs, and the bulk moduli of the crystals will be presented, and the experimental LTEC values will also be listed for reference.

2. Theoretical Method

2.1. Chemical Bond Parameters. Intrinsic physical properties of crystal are determined by the constituent elements, the spatial distribution of the atoms, and the interactions among them. The last one is referred to as the chemical bond, which plays a significant role in mechanical properties such as hardness, thermal expansion, and compressibility. The chemical bond theory of dielectric description supplies an efficacious investigation method for the mechanical properties study of complex crystals from a bonding standpoint.

Suppose we have a crystal, its chemical formula is A_mB_n (A represents cation and B represents anion); in this crystal, A has i types of symmetry sites, and the number of A on site i is ai. In order to distinguish the sites, we write the chemical formula as $A^1_{a1}A^2_{a2}\cdots A^i_{ai}B^1_{b1}B^2_{b2}\cdots B^j_{bj}$, which is called the crystal formula. A^i_{ai} and B^j_{bj} represent the different constituent elements or the same element in different sites, and ai and bj represent the quantity of the corresponding element. Now, we can distinguish the chemical bond not only by the difference in component elements but also by the difference in the sites, namely, the bond length and the symmetry. When detailed crystal structural information is available, by using the following formulas, the crystal formula can be written in a linear combination of the subformulas.[18]

$$A^1_{a1}A^2_{a2}\cdots A^i_{ai}B^1_{b1}B^2_{b2}\cdots B^j_{bj} = \sum_{i,j} A^i_{mi}B^j_{nj} = \sum_{\mu} (A_mB_n)^{\mu} \tag{1}$$

$$mi = \frac{N_C(B^j - A^i) \times ai}{N_C(A^i)}, nj = \frac{N_C(A^i - B^j) \times bj}{N_C(B^j)} \tag{2}$$

$N_C(B^j - A^i)$ is the quantity of B^j ions in the coordination group of an A^i ion, and $N_C(A^i)$ is the nearest coordination number of the A^i ion. $(A_mB_n)^{\mu}$ is the so-called subformula, which represents a pseudo-binary crystal; the superscript μ indicates the species. In each pseudo-binary crystal, there is only one species of chemical bond.

For any species of chemical bond, the fractions of ionicity f^{μ}_i and covalence f^{μ}_c are evaluated from the average band gap E^{μ}_g and its heteropolar part, C^{μ}, and homopolar part, E^{μ}_h:[18−24]

$$f^{\mu}_i = \left(\frac{C^{\mu}}{E^{\mu}_g}\right)^2$$
$$f^{\mu}_c = \left(\frac{E^{\mu}_h}{E^{\mu}_g}\right)^2 \tag{3}$$

$$(E^{\mu}_g)^2 = (C^{\mu})^2 + (E^{\mu}_h)^2 \tag{4}$$

$$E^{\mu}_h = 39.74(d^{\mu})^{-2.48} \tag{5}$$

$$C^{\mu} = 14.4b^{\mu}\exp(-k^{\mu}_s r^{\mu}_0)\left[Z^{\mu}_A - \frac{n}{m}Z^{\mu}_B\right]\frac{1}{r^{\mu}_0} \quad n \geq m$$
$$C^{\mu} = 14.4b^{\mu}\exp(-k^{\mu}_s r^{\mu}_0)\left[\frac{m}{n}Z^{\mu}_A - Z^{\mu}_B\right]\frac{1}{r^{\mu}_0} \quad m \geq n \tag{6}$$

where $d^{\mu} = 2r^{\mu}_0$ is the chemical bond length in ångstroms and $\exp(-k^{\mu}_s r^{\mu}_0)$ is the Thomas−Fermi screening factor. Z^{μ}_A and Z^{μ}_B are the effective valence electron numbers of A and B ions, respectively, and b^{μ} is a structural correction factor.

2.2. Lattice Energy, LTEC, and Bulk Modulus. The lattice energy of ionic crystals is one of the most important quantities in elucidating the structure, character, and behavior of solids. Liu et al.[25] proposed a method to estimate the lattice energy of ionic crystals based on chemical bond theory.[26,27] For any type of pseudo-binary crystal $(A_mB_n)^{\mu}$, its contributions to the lattice energy $U(mn)^{\mu}$ comes from two parts: ionic part $U(mn)^{\mu}_i$ and covalent part $U(mn)^{\mu}_c$. The total lattice energy of a complex crystal is obtained by summarizing the contributions of every pseudo-binary crystal.[25]

(12) Hikichi, Y.; Ota, T.; Daimon, K.; Hattori, T.; Mizuno, M. *J. Am. Ceram. Soc.* **1998**, *81*, 2216.
(13) Hikichi, Y.; Ota, T.; Hattori, T. *Mineral. J.* **1997**, *19*, 123.
(14) Perrière, L.; Bregiroux, D.; Naitali, B.; Audubert, F.; Champion, E.; Smith, D. S.; Bernache-Assollant, D. *J. Eur. Ceram. Soc.* **2007**, *27*, 3207.
(15) Zhang, S.; Zhou, S.; Li, H.; Li, L. *Inorg. Chem.* **2008**, *47*, 7863.
(16) Li, H. L.; Zhou, S. H.; Zhang, S. Y. *J. Solid State Chem.* **2007**, *180*, 589.
(17) Trachenko, K. *J. Phys.: Condens. Matter* **2004**, *16*, R1491.
(18) Zhang, S. Y. *Chin. J. Chem. Phys.* **1991**, *4*, 109.
(19) Phillips, J. C.; Van Vechten, J. A. *Phys. Rev. Lett.* **1969**, *23*, 1115.
(20) Levine, G. *Phys. Rev. B* **2000**, *61*, 4636.
(21) Gao, F.; He, J.; Wu, E.; Liu, S.; Yu, D.; Li, D.; Zhang, S.; Tian, Y. *Phys. Rev. Lett.* **2003**, *91*, 015502.
(22) Li, L.; Zhou, S.; Zhang, S. *J. Phys. Chem. C* **2007**, *111*, 3205.
(23) Wu, Z. J.; Meng, Q. B.; Zhang, S. Y. *Phys. Rev. B* **1998**, *58*, 958.
(24) Xue, D.; Zhang, S. *J. Phys.: Condens. Matter* **1996**, *8*, 1949.
(25) Liu, D.; Zhang, S.; Wu, Z. *Inorg. Chem.* **2003**, *42*, 2465.
(26) Phillips, J. C. *Rev. Mod. Phys.* **1970**, *42*, 317.
(27) Levine, B. F. *J. Chem. Phys.* **1973**, *59*, 1463.

$$U(mn)^{\mu} = U(mn)_{\mathrm{i}}^{\mu} + U(mn)_{\mathrm{c}}^{\mu} \quad (7)$$

$$U = \sum_{\mu} U(mn)^{\mu} \quad (8)$$

The lattice energy density u^{μ} of each binary crystal is defined as[28]

$$u(mn)^{\mu} = \frac{U(mn)^{\mu}}{N_{\mathrm{AV}} n^{\mu} \upsilon_{\mathrm{b}}^{\mu}} \quad (9)$$

where N_{AV} is the Avogadro constant, n^{μ} is the quantity of one species of chemical bond in one formula unit, and $\upsilon_{\mathrm{b}}^{\mu}$ is the chemical bond volume of the species of bond, which defined as[27]

$$\nu_{\mathrm{b}}^{\mu} = \frac{(d^{\mu})^3}{\sum_{v} (d^{v})^3 N_{\mathrm{b}}^{v}} \quad (10)$$

in which N_{b}^{v} is the number of bonds per cubic centimeter.

Deep research revealed that the LTEC and the bulk modulus of simple crystals have a significant relationship with their lattice energies or lattice energy densities. For LTEC,[29]

$$\alpha = \sum_{\mu} F_{mn}^{\mu} \alpha_{mn}^{\mu} \quad (10^{-6}\ \mathrm{K}^{-1}) \quad (11)$$

$$\alpha_{mn}^{\mu} = -3.1685 + 0.8376\chi_{mn}^{\mu} \quad (10^{-6}\ \mathrm{K}^{-1}) \quad (12)$$

with the parameter χ_{mn}^{μ} linking the lattice energy of binary crystals and their LTEC together, which can be obtained from the crystal structural data and lattice energy. F_{mn}^{μ} is the fraction of one type of bond in the complex crystal. The detailed theoretical method can be found in ref 29.

In the case of the bulk modulus, the density of lattice energy $u(mn)^{\mu}$ and bulk modulus $B(mn)^{\mu}$ have a linear relationship for binary crystals,[28]

$$B(mn)^{\mu} = \delta^{\mu} + \frac{u(mn)^{\mu}}{\beta(mn)^{\mu}} \quad (13)$$

Here, δ^{μ} is a constant, $\beta(mn)^{\mu}$ represents the slopes of fitting lines, which relate to Z_{A} (chemical valence of cation) and $N_{\mathrm{C}}(\mathrm{A})$ (coordination number of cation). The bulk modulus of one complex crystal can be calculated from[30]

$$B_{\mathrm{m}} = \frac{1}{\kappa_{\mathrm{m}}} \quad (14)$$

$$\kappa_{\mathrm{m}} = \frac{1}{V_{\mathrm{m}}} \sum_{\mu} V^{\mu} \kappa_{\mu} = \frac{1}{V_{\mathrm{m}}} \sum_{\mu} \frac{V^{\mu}}{B(mn)^{\mu}} \quad (15)$$

where V^{μ} is the volume of the particular chemical bond in one formula unit. The application of this method to complex ionic and covalent crystals has also been demonstrated.[30,31] One can refer to the detailed theoretical method.

3. Results and Discussion

3.1. Structure and subformula equation. The monazite phase is a monoclinic structure, which belongs to the number 14 space group with $P2_1/n$ settings. The cell contains four formula units for a total of 24 atoms. In the cell, all of the atoms reside in the 4*e* (*x*, *y*, *z*) sites according to the Wyckoff notation. R or X atoms take only one crystallographic equivalent site, and they are 9- and 4-fold coordinated to O atoms, respectively. However, for O atoms, they take four crystallographic nonequivalent sites, which are denoted as O^1, O^2, O^3, and O^4. Among them, O^1, O^3,and O^4 are 3-fold coordinated (to two R atoms and one X atom), and the O^2 is 4-fold coordinated (to three R atoms and one X atom). According to eqs 1 and 2, the monazite-type RXO_4 can be decomposed into the following subformula equation:

$$\begin{aligned} \mathrm{RXO_4} = {} & \mathrm{R_{1/9}O_{1/3}^{1\prime}} + \mathrm{R_{1/9}O_{1/3}^{1\prime\prime}} + \mathrm{R_{1/9}O_{1/3}^{3\prime}} + \mathrm{R_{1/9}O_{1/3}^{3\prime\prime}} + \\ & \mathrm{R_{1/9}O_{1/3}^{4\prime}} + \mathrm{R_{1/9}O_{1/3}^{4\prime\prime}} + \mathrm{R_{1/9}O_{1/4}^{2\prime}} + \mathrm{R_{1/9}O_{1/4}^{2\prime\prime}} + \mathrm{R_{1/9}O_{1/4}^{2\prime\prime\prime}} + \\ & \mathrm{X_{1/4}O_{1/3}^{1}} + \mathrm{X_{1/4}O_{1/3}^{3}} + \mathrm{X_{1/4}O_{1/3}^{4}} + \mathrm{X_{1/4}O_{1/4}^{2}} = 6\mathrm{R_{1/9}O_{1/3}^{\prime}} + \\ & 3\mathrm{R_{1/9}O_{1/4}^{\prime\prime}} + 3\mathrm{X_{1/4}O_{1/3}^{\prime}} + \mathrm{X_{1/4}O_{1/4}^{\prime\prime}} \quad (16) \end{aligned}$$

The zircon phase belongs to a tetragonal structure within the number 141 ($I4_1/amd$) space group and contains four formula units for a total of 24 atoms. The R and X atoms reside in special Wyckoff sites, namely, 4*a* (0, 3/4, 1/8) and 4*b* (0, 1/4, 3/8), respectively. The R atoms are 8-fold coordinated, and the X atoms are 4-fold coordinated to O atoms. All of the O atoms reside in the 16*h* (0, *y*, *z*) site and coordinate to two R atoms and one X atom. The zircon-type RXO_4 can be decomposed as follows:

$$\mathrm{RXO_4} = \mathrm{R_{1/2}O_{4/3}^{\prime}} + \mathrm{R_{1/2}O_{4/3}^{\prime\prime}} + \mathrm{XO_{4/3}} \quad (17)$$

From the structural parameters, one can find that the structures of monazite (Figure 1A) and zircon (Figure 1B) mainly differ in the coordination number of R, namely, 9 in

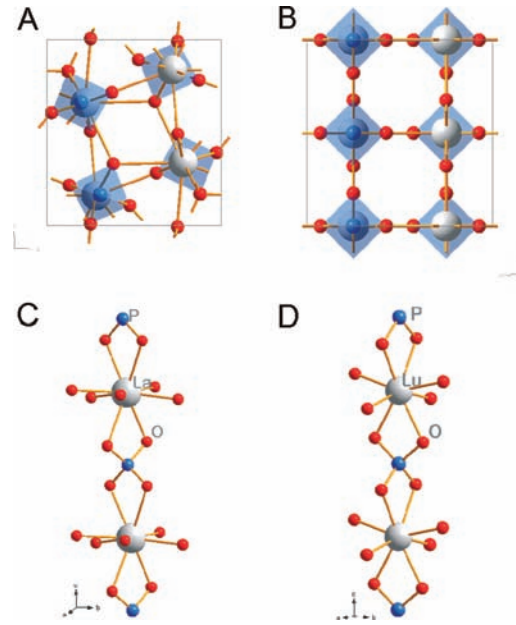

Figure 1. The crystal structure of RXO_4 in (A) monazite and (B) zircon phases. C and D show the atomic chains along the *c* axis in monazite and zircon, respectively. The biggest white spheres are rare earth, R; the medium blue ones are P or As, and the smallest red ones are O.

(28) Zhang, S.; Li, H.; Zhou, S.; Cao, X. *J. Phys. Chem. B* **2007**, *111*, 1304.
(29) Zhang, S. Y.; Li, H. L.; Zhou, S. H.; Pan, T. Q. *Jpn. J. Appl. Phys.* **2006**, *45*, 8801.
(30) Zhang, S.; Li, H.; Li, L.; Zhou, S. *Appl. Phys. Lett.* **2007**, *91*, 251905.
(31) Zhang, S.; Li, H.; Li, H.; Zhou, S.; Cao, X. *J. Phys. Chem. B* **2007**, *111*, 1304.

Table 1. Chemical Bond Parameters, LTEC, and Bulk Modulus of $LaPO_4$ Crystals[a]

bond (n^μ)	d^μ	f_c^μ	U^μ/n^μ	v_b^μ	α^μ	B_m^μ
La−$O^{1\prime}$ (1)	2.480	0.1600	595	6.876	10.27	184.0
La−$O^{1\prime\prime}$ (1)	2.554	0.1585	581	7.510	10.60	164.6
La−$O^{3\prime}$ (1)	2.503	0.1595	591	7.069	10.37	177.7
La−$O^{3\prime\prime}$ (1)	2.616	0.1575	570	8.070	10.87	150.3
La−$O^{4\prime}$ (1)	2.466	0.1603	598	6.760	10.21	188.0
La−$O^{4\prime\prime}$ (1)	2.548	0.1586	582	7.457	10.57	166.1
La−O′ (6)	**2.528**	**0.1591**	**586**	**7.291**	**10.48**	**170.0**
La−$O^{2\prime}$ (1)	2.588	0.0755	606	7.814	11.13	98.7
La−$O^{2\prime\prime}$ (1)	2.671	0.0749	591	8.590	11.51	87.6
La−$O^{2\prime\prime\prime}$ (1)	2.783	0.0741	571	9.717	12.01	75.0
La−O″ (3)	**2.681**	**0.0748**	**589**	**8.707**	**11.55**	**85.2**
P−O^1 (1)	1.523	0.4333	6135	1.592	0.87	1015.8
P−O^3 (1)	1.541	0.4321	6088	1.650	0.90	973.4
P−O^4 (1)	1.537	0.4323	6098	1.637	0.89	982.6
P−O′ (3)	**1.534**	**0.4326**	**6107**	**1.626**	**0.89**	**990.0**
P−O^2 (1)	1.553	0.2904	6920	1.688	0.92	1093.9
P−O″ (1)	**1.553**	**0.2904**	**6920**	**1.688**	**0.92**	**1093.9**

[a] Bond length d^μ in Å, lattice energy U^μ in kJ mol^{-1}, LTEC α^μ in 10^{-6} K^{-1}, bulk modulus B_m^μ in GPa, and the bond volume v_b^μ in Å^3.

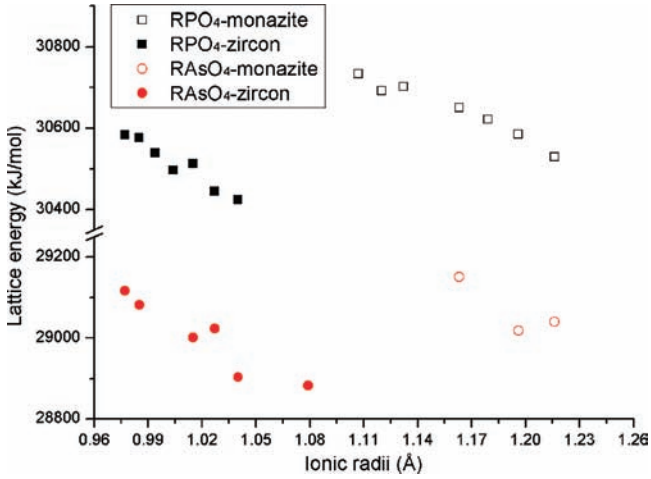

Figure 2. The variation of the lattice energy with the ionic radii of the lanthanides in the RXO_4 (R = lanthanides; X = P, As) series.

the monazite (Figure 1C) and 8 in the zircon (Figure 1D), the symmetry and the relative position between $RO_{9(8)}$ and XO_4 polyhedra.

3.2. Chemical Bond Parameters. As has been mentioned previously, in the monazite structure, the R atoms are 9-fold coordinated and the X atoms are 4-fold coordinated; there are 13 kinds of bonds in the crystal. The calculated chemical bond parameters of $LaPO_4$ are shown in Table 1. From the calculated chemical bond parameters, we can find that all of the La−O bonds are ionic dominated, whereas the covalent fractions of P−O bonds are very high, namely, 0.29−0.43. Furthermore, both the La−O and P−O bonds can be grossly divided into two groups: One contains the La−O′ and P−O′ groups, in which the O′ (O^1, O^3, O^4) atoms are 3-fold coordinated and the covalent fractions are 0.16 and 0.43, respectively. The other contains the La−O″ and P−O″ groups, in which the O″ (O^2) atoms are 4-fold coordinated and their covalent fractions are lower, 0.07 for the La−O″ and 0.29 for the P−O″ bond. This indicates that the covalent fractions depend strongly on the coordination number of O. This can be easily understood from the viewpoint of electron distribution: the valence charge of O atoms is distributed

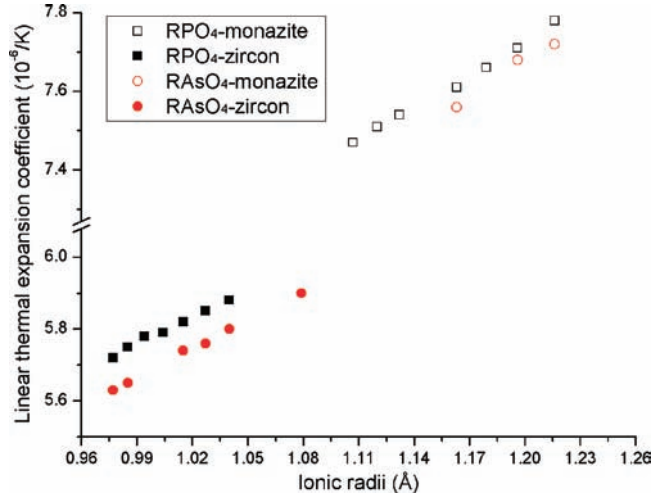

Figure 3. The variation of the linear thermal expansion coefficient with the ionic radii of the lanthanides in the RXO_4 (R = lanthanides; X = P, As) series.

averagely on every bond; therefore, for a given bond length, those bonds with 3-fold coordinated O must have higher valence charge density. As a result, they have a lower heteropolar gap C^μ, and then lower covalent fractions than those bonds with 4-fold coordinated O. Other RXO_4 in monazite structures have similar chemical bond parameters to that of $LaPO_4$; for the sake of simplcity, we just show the mean values of the two groups in Table 2.

In the zircon structure, the situation is rather simple: the rare earths are 8-fold coordinated with two kinds of bond lengths, and the P (or As) is 4-fold coordinated with only one kind of bond. The covalent fractions are about 0.160 for R−O, 0.373 for P−O, and 0.356 for As−O bonds (Table 3).

The bonding characteristics of zircon−RVO_4 have been reported previously.[15] Through the zircon structure, the covalency of R−O bonds vary slightly from La to Lu in a given series, or between different series. While the covalent

(32) Shannon, R. *Acta Crystallogr., Sect. A* **1976**, *32*, 751.
(33) Armbruster, A. *J. Phys. Chem. Solids* **1976**, *37*, 321.
(34) Mogilevsky, P.; Zaretsky, E.; Parthasarathy, T.; Meisenkothen, F. *Phys. Chem. Miner.* **2006**, *33*, 691.
(35) Errandonea, D.; Pellicer-Porres, J.; Manjón, F. J.; Segura, A.; Ferrer-Roca, C.; Kumar, R. S.; Tschauner, O.; Rodríguez-Hernández, P.; López-Solano, J.; Radescu, S.; Mujica, A.; Muñoz, A.; Aquilanti, G. *Phys. Rev. B* **2005**, *72*, 174106.
(36) Yunxiang, N.; Hughes, J. M.; Mariano, A. N. *Am. Mineral.* **1995**, *80*, 21.
(37) Schmidt, M.; Müller, U.; Gil, R. C.; Milke, E.; Binnewies, M. *Z. Anorg. Allg. Chem.* **2005**, *631*, 1154.
(38) Kolitsch, U.; Holtstam, D.; Gatedal, K. *Eur. J. Mineral.* **2004**, *16*, 111.
(39) Schopper, H. C.; Urban, W.; Ebel, H. *Solid State Commun.* **1972**, *11*, 955.
(40) Kahle, H. G.; Schopper, H. C.; Urban, W.; Wüchner, W. *Phys. Status Solidi B* **1970**, *38*, 815.
(41) Rasmussen, S. E.; Jørgensen, J.-E.; Lundtoft, B. *Powder Diffr.* **1993**, *8*, 164.
(42) Milligan, W. O.; Mullica, D. F.; Beall, G. W.; Boatner, L. A. *Inorg. Chim. Acta* **1982**, *60*, 39.
(43) Guillot-Noël, O.; Kahn-Harari, A.; Viana, B.; Vivien, D.; Antic-Fidancev, E.; Porcher, P. *J. Phys.: Condens. Matter* **1998**, *10*, 6491.
(44) Kang, D.-H.; Schleid, T. *Z. Anorg. Allg. Chem.* **2005**, *631*, 1799.
(45) Long, F. G.; Stager, C. V. *Can. J. Phys.* **1977**, *55*, 1633.
(46) Kang, D.-H.; Hoss, P.; Schleid, T. *Acta Crystallogr., Sect. E* **2005**, *61*, i270.

Table 2. Chemical Bond Parameters, LTEC, and Bulk Modulus of RXO_4 Crystals within the Monazite Structure[a]

crystal	bond (n^μ)	$\overline{d^\mu}$	$\overline{f_c^\mu}$	$\overline{U^\mu/n^\mu}$	$\overline{\nu_b^\mu}$	$\overline{\alpha^\mu}$	$\overline{B_m^\mu}$	U	α	α_{exp}	B_m
$LaPO_4$[b]	La−O′ (6)	2.528	0.1591	586	7.291	10.48	170.0	30529	7.78	7.5[10]	134.0
	La−O″ (3)	2.681	0.0748	589	8.707	11.55	85.2			10.5[10]	
	P−O′ (3)	1.534	0.4326	6107	1.626	0.89	990.0			10.0[13]	
	P−O″ (1)	1.553	0.2904	6920	1.688	0.92	1093.9				
$CePO_4$[b]	Ce−O′ (6)	2.501	0.1592	591	7.089	10.37	176.3	30585	7.71	9.9[13]	137.2
	Ce−O″ (3)	2.664	0.0747	593	8.586	11.48	86.5				
	P−O′ (3)	1.535	0.4317	6105	1.636	0.89	984.4				
	P−O″ (1)	1.546	0.2901	6942	1.672	0.91	1108.0				
$PrPO_4$[b]	Pr−O′ (6)	2.484	0.1592	595	6.960	10.29	180.6	30622	7.66		139.7
	Pr−O″ (3)	2.651	0.0747	595	8.485	11.42	87.6				
	P−O′ (3)	1.533	0.4313	6110	1.635	0.89	985.3				
	P−O″ (1)	1.547	0.2896	6940	1.680	0.91	1102.9				
$NdPO_4$[b]	Nd−O′ (6)	2.467	0.1592	598	6.843	10.22	184.7	30650	7.61	9.8[13]	142.3
	Nd−O″ (3)	2.638	0.0746	597	8.387	11.36	88.9				
	P−O′ (3)	1.534	0.4306	6110	1.642	0.89	981.4				
	P−O″ (1)	1.547	0.2891	6941	1.685	0.91	1099.6				
$SmPO_4$[b]	Sm−O′ (6)	2.439	0.1595	603	6.630	10.10	192.3	30702	7.54	9.7[13]	146.0
	Sm−O″ (3)	2.618	0.0747	601	8.234	11.27	90.3				
	P−O′ (3)	1.535	0.4300	6106	1.651	0.89	975.3				
	P−O″ (1)	1.541	0.2890	6960	1.670	0.90	1112.5				
$EuPO_4$[b]	Eu−O′ (6)	2.430	0.1596	605	6.561	10.06	194.9	30692	7.51		147.1
	Eu−O″ (3)	2.612	0.0747	603	8.197	11.24	90.5				
	P−O′ (3)	1.537	0.4295	6101	1.660	0.89	969.1				
	P−O″ (1)	1.545	0.2884	6949	1.685	0.91	1100.5				
$GdPO_4$[b]	Gd−O′ (6)	2.413	0.1596	609	6.446	9.98	199.7	30734	7.47		149.0
	Gd−O″ (3)	2.603	0.0745	604	8.142	11.20	91.2				
	P−O′ (3)	1.538	0.4288	6100	1.669	0.89	963.6				
	P−O″ (1)	1.538	0.2883	6970	1.668	0.89	1115.4				
$LaAsO_4$[c]	La−O′ (6)	2.542	0.1554	583	7.634	10.55	161.3	29040	7.72		124.5
	La−O″ (3)	2.715	0.0729	584	9.366	11.71	76.3				
	As−O′ (3)	1.680	0.4178	5749	2.203	0.49	690.3				
	As−O″ (1)	1.695	0.2786	6541	2.261	0.50	774.2				
$CeAsO_4$[d]	Ce−O′ (6)	2.522	0.1557	587	7.469	10.47	165.9	29018	7.68		125.1
	Ce−O″ (3)	2.709	0.0729	585	9.345	11.68	75.5				
	As−O′ (3)	1.692	0.4169	5721	2.253	0.50	671.9				
	As−O″ (1)	1.682	0.2788	6576	2.212	0.48	795.2				
$NdAsO_4$[c]	Nd−O′ (6)	2.483	0.1560	594	7.157	10.30	175.4	29151	7.56		130.6
	Nd−O″ (3)	2.672	0.0730	592	9.027	11.52	78.1				
	As−O′ (3)	1.681	0.4167	5749	2.217	0.49	686.0				
	As−O″ (1)	1.688	0.2780	6562	2.244	0.49	782.2				

[a] n^μ is the number of the μth-type chemical bond in one formula unit. Bond length $\overline{d^\mu}$ in Å and lattice energy U^μ and U in kJ mol^{-1}; LTEC α^μ, α, and α_{exp} in 10^{-6} K^{-1}; α_{exp} is the experimental value. Bulk modulus $\overline{B_m^\mu}$ and B_m in GPa, and the bond volume $\overline{v_b^\mu}$ in Å^3. [b] Structure after Yunxiang et al.[36] [c] Structure after Schmidt et al.[37] [d] Structure after Kolitsch et al.[38]

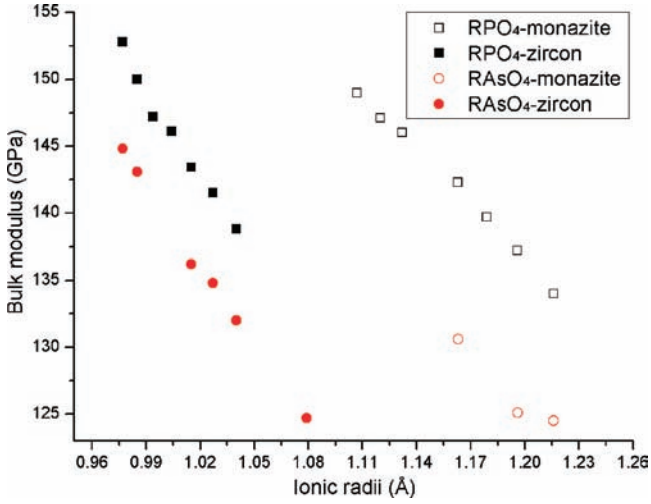

Figure 4. The variation of the bulk modulus with the ionic radii of the lanthanides in the RXO_4 (R = lanthanides; X = P, As) series.

fractions of X−O decrease in the order f_c^{P-O} (0.3730) > f_c^{As-O} (0.3555) > f_c^{V-O} (0.3538),[15] which is consistent with the ionic radii and electronegative orders of X, namely, R_i^V (0.355) > R_i^{As} (0.335) > R_i^P (0.170)[32] and χ^V (1.9) < χ^{As} (2.0) < χ^P (2.1). With the decreasing of ionic radii and increasing of electronegativity, the polarizability of X increased; therefore, an increasing of covalency of X−O bonds was observed when X went from V, to As, and to P.

3.3. Lattice Energy, LTEC, and Bulk Modulus. We calculated the lattice energies, LTECs, and bulk moduli of the bonds on the basis of the chemical bond parameters, as listed in Tables 2 and 3. In both monazite and zircon structures, the chemical valence of X (+5) is higher than that of R (+3), and the bond length of X−O is shorter than that of R−O. As a result, the X−O bonds have higher interaction potential than the R−O bonds. The calculated lattice energy agrees with the result very well: X(= P, As, V)−O bonds make quite large contributions to the lattice energy relative to R−O bonds. And furthermore, in the zircon structure, the lattice energy of X−O bonds decreases in the order $U^{V-O} < U^{As-O} < U^{P-O}$, and so do the bulk modulus and LTEC.

The extremely high lattice energy of P−O (or As−O or V−O) bonds means that the PO_4 (or AsO_4 or VO_4) tetrahedra

(47) Lohmuller, G.; Schmidt, G.; Deppisch, B.; Gramlich, V.; Scheringer, C. *Acta Crystallogr., Sect. B* **1973**, *29*, 141.

Table 3. Chemical Bond Parameters, LTEC, and Bulk Modulus of RXO_4 Crystals within the Zircon Structure[a]

crystal	bond (n^μ)	d^μ	f_c^μ	U^μ/n^μ	v_b^μ	α^μ	B_m^μ	U	α	α_{exp}	B_m	B_{ref}
$ScPO_4$[b]	Sc−O′ (4)	2.153	0.1644	768	6.187	9.73	173.9	30782	6.95	5.53[39]	175.1	
	Sc−O″ (4)	2.270	0.1600	736	7.252	10.28	142.5					
	P−O (4)	1.534	0.3699	6191	2.238	0.83	731.6					
YPO_4[c]	Y−O′ (4)	2.300	0.1608	729	7.419	9.46	137.9	30404	6.70	6.26,5.90[39]	144.4	132[34]
	Y−O″ (4)	2.373	0.1585	711	8.148	9.78	122.6			6.27,5.87[40]		145[35]
	P−O (4)	1.544	0.3721	6161	2.244	0.85	726.0			6.2[12]		
$TbPO_4$[d]	Tb−O′ (4)	2.331	0.1607	721	7.657	8.27	132.3	30424	5.88		138.8	
	Tb−O″ (4)	2.399	0.1587	705	8.347	8.54	118.7					
	P−O (4)	1.536	0.3744	6180	2.191	0.84	745.7					
$DyPO_4$[d]	Dy−O′ (4)	2.317	0.1607	725	7.553	8.22	134.7	30445	5.85		141.5	
	Dy−O″ (4)	2.385	0.1586	708	8.238	8.49	120.8					
	P−O (4)	1.537	0.3735	6178	2.205	0.84	740.9					
$HoPO_4$[d]	Ho−O′ (4)	2.307	0.1612	727	7.445	8.18	137.2	30512	5.82		143.4	
	Ho−O″ (4)	2.379	0.1590	710	8.164	8.46	122.2					
	P−O (4)	1.532	0.3742	6191	2.180	0.83	750.7					
$ErPO_4$[d]	Er−O′ (4)	2.288	0.1616	732	7.274	8.11	141.3	30496	5.79	6.0[12]	146.1	
	Er−O″ (4)	2.373	0.1590	711	8.115	8.44	123.1					
	P−O (4)	1.536	0.3736	6181	2.201	0.84	742.6					
$TmPO_4$[d]	Tm−O′ (4)	2.286	0.1615	733	7.264	8.10	141.5	30539	5.78		147.2	
	Tm−O″ (4)	2.365	0.1591	713	8.044	8.41	124.5					
	P−O (4)	1.533	0.3736	6189	2.191	0.83	746.9					
$YbPO_4$[d]	Yb−O′(4)	2.271	0.1618	737	7.136	8.04	144.8	30576	5.75	6.0[12]	150.0	
	Yb−O″ (4)	2.355	0.1592	715	7.957	8.37	126.3					
	P−O (4)	1.532	0.3733	6192	2.191	0.83	747.4					
$LuPO_4$[d]	Lu−O′ (4)	2.257	0.1620	740	7.025	7.99	147.8	30583	5.72	6.2[12]	152.8	166[33]
	Lu−O″ (4)	2.344	0.1592	718	7.869	8.33	128.2					
	P−O (4)	1.534	0.3726	6188	2.205	0.83	741.8					
$ScAsO_4$[e]	Sc−O′ (4)	2.140	0.1617	771	6.268	9.68	172.4	29324	6.87	5.83[39]	166.0	
	Sc−O″ (4)	2.312	0.1553	725	7.904	10.49	128.9					
	As−O (4)	1.680	0.3532	5835	3.032	0.43	511.1					
$YAsO_4$[f]	Y−O′ (4)	2.300	0.1576	728	7.646	9.47	133.8	29165	6.61	6.27,6.56[39]	137.0	135[35]
	Y−O″ (4)	2.412	0.1542	702	7.818	9.96	111.8			6.23,6.57[40]		
	As−O (4)	1.667	0.3573	5861	2.911	0.42	534.5					
$SmAsO_4$[g]	Sm−O′(4)	2.359	0.1568	714	8.168	8.39	122.9	28883	5.90		124.7	
	Sm−O″ (4)	2.480	0.1535	686	9.490	8.87	101.7					
	As−O (4)	1.683	0.3582	5821	2.966	0.44	521.2					
$TbAsO_4$[h]	Tb−O′ (4)	2.318	0.1569	724	7.832	8.23	129.8	28904	5.80		132.0	
	Tb−O″ (4)	2.439	0.1534	695	9.123	8.71	107.2					
	As−O (4)	1.690	0.3558	5807	3.035	0.45	508.3					
$DyAsO_4$[h]	Dy−O′(4)	2.305	0.1574	727	7.699	8.18	132.7	29023	5.76		134.8	
	Dy−O″ (4)	2.426	0.1538	698	8.976	8.66	109.4					
	As−O (4)	1.680	0.3564	5830	2.981	0.44	519.5					
$HoAsO_4$[e]	Ho−O′ (4)	2.294	0.1576	730	7.599	8.14	134.9	29001	5.74		136.2	
	Ho−O″ (4)	2.422	0.1537	699	8.943	8.64	109.9					
	As−O (4)	1.684	0.3559	5821	3.006	0.44	514.4					
$YbAsO_4$[i]	Yb−O′ (4)	2.258	0.1582	739	7.289	8.00	142.3	29082	5.65		143.1	
	Yb−O″ (4)	2.391	0.1540	706	8.655	8.52	114.7					
	As−O (4)	1.683	0.3549	5825	3.018	0.44	512.6					
$LuAsO_4$[j]	Lu−O′ (4)	2.248	0.1585	742	7.194	7.96	144.7	29117	5.63		144.8	
	Lu−O″ (4)	2.385	0.1541	708	8.591	8.50	115.8					
	As−O (4)	1.681	0.3550	5830	3.008	0.44	514.8					

[a] n^μ is the number of the μ-type chemical bond in one formula unit. Bond length d^μ in Å and lattice energy U^μ and U in kJ mol^{-1}; LTEC α^μ, α, and α_{exp} in 10^{-6} K^{-1}; α_{exp} is the experimental value. Bulk modulus B_m^μ, B_m,and B_{ref} in GPa, and the bond volume v_b^μ in Å^3. [b] Structure after Rasmussen et al.[41] [c] Structure after Milligan et al.[42] [d] Structure after Ni et al.[36] [e] Structure after Schmidt et al.[37] [f] Structure after Guillot-Noël et al.[43] [g] Structure after Kang et al.[44] [h] Structure after Long et al.[45] [i] Structure after Kang et al.[46] [j] Structure after Lohmuller et al.[47]

are bonded very tightly; one can expect that they will be hardly deformed when the crystal is heated or under pressure. This is verified by the LTEC and bulk modulus calculations. The LTECs are lower than 1.0×10^{-6} K^{-1} and 0.5×10^{-6} K^{-1} for P−O and As−O bonds, respectively; contrarily, they are quite large for R−O bonds, namely, $(8-12) \times 10^{-6}$ K^{-1}. Significant anisotropy of LTEC in zircon structural RXO_4, especially in the vanadates, has been observed by using X-ray diffraction. This should be correlated with the great discrepancy of LTEC between R−O and X−O bonds, and the nonuniform distribution of these bonds along different axes.

The variations of the lattice energy, LTEC, and bulk modulus with the ionic radii of lanthanides are plotted in Figures 2−4. For the zircon and monazite phases, 8- and 9-fold coordination ionic radii of R are used,[32] respectively. As has been demonstrated: (1) In both monazite and zircon structures, the lattice energies, LTECs, and bulk moduli of RPO_4 and $RAsO_4$ vary linearly with the ionic radii of lanthanides, and similar trends were also found in the zircon-type RVO_4. (2) In both structures, the lattice energies of RPO_4 are larger than those of $RAsO_4$; this difference mainly resulted from the contributions of XO_4 tetrahedra. (3) In a given series (RPO_4 or $RAsO_4$), there are sudden changes in the lattice energy, LTEC, and bulk modulus. When the structure varies from zircon to monazite, crystals in the monazite structure have larger lattice energies than those in the zircon structure; this is ascribed to the higher coordination number of R in monazite than in zircon. As a consequence, the LTEC and bulk modulus of monazite are larger than those of zircon. (4) The bulk modulus and LTEC of the crystal approach that of R−O bonds rather than that of X−O bonds

because of the large bond volume of R−O compared to X−O bonds.

The experimental values of LTEC are listed in the tables for reference. One can find that, for the zircon structure, the calculated values agree well with the experimental values; for example, the calculated LTEC values of zircon range from 5.6×10^{-6} K^{-1} to 7.0×10^{-6} K^{-1}, and the experimental value is around 6.0×10^{-6} K^{-1}. As for those crystals in the monazite structure, fewer experimental values are available. Morgan and Marshall[10] reported LTEC values of $LaPO_4$ at 300 and 1300 K; they are 7.5×10^{-6} K^{-1} and 10.5×10^{-6} K^{-1}, respectively. We give a value of 7.78×10^{-6} K^{-1}. Hikichi et al.[12] reported experimental values of RPO_4 (R = La, Ce, Nd, and Sm) at 1300 K, which were in the range of $(9.7-10.0) \times 10^{-6}K^{-1}$, and they are consistent with the ones reported by Morgan and Marshall.[10] On the other hand, the calculated values are lesser than those values estimated by the dilatometer method, which agree well with the results obtained from the X-ray method, because the X-ray method calculates LTEC from the variation of cell parameters with the temperature, while the dilatometer method estimates the LTEC from the macro size variation of the specimen with temperature. As for the LTEC of $NdPO_4$ reported by Perriere et al.,[14] the X-ray method had a value of 9.41×10^{-6} K^{-1}, and the dilatometer method gave a value of 10.7×10^{-6} K^{-1}. The defect and grain boundary in the specimen will result in a overestimated value of the LTEC. For the monazite-RPO_4, the calculated results show that, with the decreasing of lanthanide ionic radii, the LTEC of the lattice decreases. This is consistent with the result reported by Hikichi et al.[13] for R on going from La to Sm, while it contradicts that reported by Perriere et al.[14] (R going from La to Gd). This divergence might result from the specimen preparation and measurement.

A few experimental bulk modulus values of zircon-type RPO_4 were reported, including LuPO4, reported by Armbruster.[33] Its bulk modulus is 166 GPa, with our calculations giving a value of 152.8 GPa. And for YPO_4, the measured value is 132 GPa,[34] and the calculated value is 144.4 GPa. As can be seen, the calculated values agree well with the experimental values. In addition, Errandonea et al.[35] estimated the bulk modulus values of YPO_4 and $YAsO_4$ by using the formal chemical valence of Y and the bond length of Y−O, and this yielded 145 and 135 GPa, respectively. They are in agreement with our calculated values, namely, 144.4 and 137.7 GPa for YPO_4 and $YAsO_4$, respectively.

4. Conclusion

The chemical bond characteristics, thermal expansibility, and compressibility of RPO_4 and $RAsO_4$ within monazite and zircon structures were systematically investigated. The R−O bonds are ionically dominated and change slightly with the variation of R due to the lanthanide contraction. The covalency fractions of X−O bonds are relatively high and vary with the ionic radii and electronegativity of X. In both the monazite and zircon structures, the lattice energies, LTECs, and bulk moduli of RPO_4 and $RAsO_4$ vary linearly with the ionic radii of lanthanides. The XO_4 tetrahedra have high lattice energies and therefore behave nearly rigidly during deformation. The LTEC and bulk modulus of a crystal are determined by the R−O bonds, because the R−O bonds have larger bond volumes than X−O bonds.

IC900337J